LAWRENCE
LIVERMORE
NATIONAL
LABORATORY

UCRL-JRNL-209163

Electron Broadening of Isolated Lines with Stationary Non-Equilibrium Level Populations

C. A. Iglesias

January 24, 2005

High Energy Density Physics

Electron broadening of isolated lines with stationary non-equilibrium level populations

Carlos A. Iglesias
Lawrence Livermore National Laboratories
P.O. Box 808, Livermore, CA 94550, USA

It is shown that a quantum kinetic theory approach to line broadening, extended to stationary non-equilibrium states, yields corrections to the standard electron impact widths of isolated lines that depend on the population of the radiator internal levels. A consistent classical limit from a general quantum treatment of the perturbing electrons also introduces corrections to the isolated line widths. Both effects are essential in preserving detailed-balance relations. Preliminary analysis indicates that these corrections may resolve existing discrepancies between theoretical and experimental widths of isolated lines. An experimental test of the results is proposed.

PACS number(s): 32.70Jz, 52.25Os

1. INTRODUCTION

The Stark broadening of spectral lines provides a valuable diagnostic tool as well as a probe to study the interface between atomic and plasma physics. Therefore, it is crucial to validate line-broadening theories with well-characterized experiments. To this end experiments measuring the *2p-2s* and *3p-3s* line profiles in the Li- and Be-like series of elements ranging from Be to Ne generated valuable data. [1-9] There are two important features of these transitions. Firstly, they involve simple atomic systems making full quantum mechanical calculations tractable. Secondly, the ion broadening is small. [9] Consequently, these transitions afford tests of electron line broadening theories and the underlying electron-ion collision processes in plasmas.

There is clear evidence indicating significant discrepancies between experiment and theory for these isolated lines. [1-13] Recent quantum mechanical calculations of the electron Stark widths corroborated earlier theoretical results and did not resolve the discrepancies. [10-13] The latest version of the non-perturbative semi-classical method [14] is also in good agreement with the quantum mechanical results. Therefore, the discrepancies are probably not due to numerical inaccuracies. On the other hand, an alternative interpretation of the experiments was proposed; [10] however, different experiments using distinct plasma sources have obtained consistent line width measurements decreasing the possibility of large systematic experimental errors. [1-9]

A possible explanation is the failure of some approximations in the standard impact theory [15] employed in the line width calculations. [1,10-14] Indeed, the standard impact theory assumes classical thermal averages and neglects initial correlations between radiator and perturbers at the onset of the theoretical development. The purpose here is to show that the quantum kinetic theory method to line broadening, [16,17] extended to stationary non-equilibrium systems, yields corrections to the standard impact theory of isolated lines.

In the kinetic theory approach the neglect of initial correlations is not formally necessary and is only introduced to compare with previous theories or to simplify calculations. As a result, there are radiator level population dependent terms absent in the standard impact theory. A consistent classical limit from a quantum treatment of the perturbing electrons also introduces corrections to the width. Both effects are essential for satisfying detailed-balance relations. Preliminary application of these corrections to past experiments suggests possible resolution to the above discrepancies. Finally, experiments are proposed to test their validity.

The organization of the paper is as follows. The main results from the kinetic theory method for isolated lines are summarized in Section 2. The formalism is applied to a two-level radiator in Section 3 and contact is made with the standard impact theory in Section 4. The experimental consequences are discussed in Section 5 with conclusions in Section 6.

2. FORMALISM

The starting point is the quantum kinetic theory of time correlation functions applied to line broadening. [16,17] This method confirmed anticipated results in plasma line broadening that were previously introduced through *ad hoc* assumptions. Here the kinetic theory approach is extended to obtained second-order width expressions for radiators with stationary non-equilibrium internal level populations typical of experiments.

2.1 Radiator-perturber system

The assumed system consists of a single radiator (emitting or absorbing atom or ion) immersed in an electron gas. In the experiments the electron gas is well described by a Maxwellian velocity distribution at a local temperature. The electrons in the radiator internal states, however, are often not in thermal equilibrium with the perturbing electron gas. In these situations the experimental apparatus (e.g.; the gas-liner pinch [2-6] or low pressure pulsed arc

[7-9]) provides an external field that constrains the plasma from reaching thermal equilibrium. No specific assumptions are made about this external field except that during the measurements it is time independent so that the system relaxes to a stationary non-equilibrium state and it does not interact with the radiator internal degrees of freedom.

For stationary conditions

$$\frac{\partial \rho}{\partial t} = -i\hbar^{-1}\left[H,\rho\right] = L\rho = 0 \tag{2.1.1}$$

with ρ, H, and L the density matrix, Hamiltonian, and Liouville operators for the system, respectively, and $\left[\cdots,\cdots\right]$ the commutator operation. Expanding the density matrix in terms of orthonormal Hamiltonian eigenstates $\left\{\left|\psi_j\right\rangle\right\}$ with eigenvalues $\left\{E_j\right\}$ where j ranges over the complete set leads to

$$\left\langle \psi_j \left| \rho(t) \right| \psi_{j'} \right\rangle = \left\langle \psi_j \left| e^{Lt} \rho(t=0) \right| \psi_{j'} \right\rangle = e^{-i\left(E_j - E_{j'}\right)t/\hbar} \left\langle \psi_j \left| \rho(0) \right| \psi_{j'} \right\rangle \quad . \tag{2.1.2}$$

A stationary state occurs when all off-diagonal matrix elements of $\rho(0)$ between non-degenerate energy levels vanish. For degenerate energy levels the diagonalization is done simultaneously for eigenstates of H and additional invariants of the motion. Furthermore, the diagonal matrix elements of $\rho(0)$ give the populations of the energy eigenstates.

2.2 Kinetic theory

The line shape function at photon energy $\hbar\omega$, neglecting ion and Doppler broadening, is written as [16]

$$\begin{aligned} I(\omega) &= \pi^{-1}\,\mathrm{Re}\int_o^\infty dt e^{i\omega t}\left\langle \vec{d}\cdot\vec{d}(t)\right\rangle \\ &= -\pi^{-1}\,\mathrm{Im}Tr_a\,\vec{d}\cdot\left\{\Delta\omega - B(a) - M(a,\omega)\right\}^{-1} f(a)\vec{d} \end{aligned} \tag{2.2.1}$$

where $\langle\cdots\rangle$ denotes an ensemble average, Tr_a a trace over the radiator internal states, and $f(a)$ the reduced distribution function for those states. Also, $\vec{d}$ is the radiator dipole operator,

$$\Delta\omega = \omega - L(a) \quad , \tag{2.2.2}$$

$$L(a) = i\hbar^{-1}\left[H(a),\cdots\right] \quad , \tag{2.2.3}$$

with $H(a)$ the internal degrees of freedom Hamiltonian for the isolated radiator. The "width and shift" operator, $B(a) + M(a,\omega)$, is expressed as a generalized binary collision by a single perturbing electron. [16] The many-body aspects are contained in reduced distribution functions, screened radiator-electron interactions, mean field terms, and multiple collision effects appearing in its definition. No approximations are made in obtaining this expression, except it was assumed that the reduced distribution functions, $f(a,1,\ldots,s)$, satisfy the equilibrium hierarchy equations. [16] Consequently, the results are not necessarily applicable to non-equilibrium states.

2.3 Second-order theory

An exact expression for $M(a,\omega)$ that takes advantage of the stationary property in Eq. (2.1.1) but does not invoke thermal equilibrium is given by [18]

$$M(a,\omega) = Tr_p L_I \rho\left\{(\omega - L)^{-1}\left[Tr_p \rho(\omega - L)^{-1}\right]^{-1} - f^{-1}(a)\right\} \quad . \tag{2.3.1}$$

where Tr_p denotes a trace over the electron gas plus the apparatus external field and L_I the Liouville operator corresponding to the radiator interaction with the electron gas excluding the radiator net charge.

A second order expansion in the radiator-electron interaction is obtained by noting that for

$$\omega - L = \Delta\omega - L_I - L_p \quad , \tag{2.3.2}$$

then

$$(\omega - L)^{-1} = (\Delta\omega - L_p)^{-1}\left\{1 + L_I(\Delta\omega - L_p)^{-1}\right\} + O(L_I^2) \tag{2.3.3}$$

where L_p is the Liouville operator for an electron gas interacting with the net radiator charge plus external field. Substitution of Eq. (2.3.3) into Eq. (2.3.1) leads to

$$M^{(2)}(a,\omega) = n_e Tr_1 L_I(a,1)\{\Delta\omega - L_o(1)\}^{-1} f_o(a) f_o(1) L_I(a,1) f_o^{-1}(a) \tag{2.3.4}$$

where n_e is the perturbing electron number density and Tr_1 denotes a trace over a single perturbing electron. For simplicity an ideal electron gas was assumed. Use was also made of the fact that the domain of $M(a,\omega)$ is in the radiator subspace. Here,

$$L_o(1) = i\hbar^{-1}[H_o(1),\cdots] \quad , \tag{2.3.5}$$

$$L_I(a,1) = i\hbar^{-1}[V(a,1),\cdots] \quad , \tag{2.3.6}$$

with $H_o(1)$ the perturbing one-electron Hamiltonian and $V(a,1)$ the radiator interaction with a single perturbing electron where both exclude the interaction with the radiator net charge.

The distribution functions appearing in Eq. (2.3.4) are zeroth-order in the interactions. In thermal equilibrium (LTE)

$$\begin{aligned} f_o(1) &\propto \exp\{-H_o(1)/T\} \quad , \\ &\qquad \text{(LTE)} \\ f_o(a) &\propto \exp\{-H(a)/T\} \quad , \end{aligned} \tag{2.3.7}$$

with T the temperature in energy units. Otherwise, $f_o(a)$ is the time independent function describing the steady-state radiator internal state populations and is a functional of $H(a)$. Equation (2.3.4) is identical to the second-order expression in Ref. 16 for non-interacting perturbers. However, the agreement may not continue to higher order expressions.

A tetradic matrix representation may be obtained by taking matrix elements between radiator eigenstates of $H(a)$ leading to

$$\langle\alpha|M(a,\omega)Y(a)|\beta\rangle = \sum_{\alpha'\beta'} M_{\alpha\beta,\alpha'\beta'}(\omega)\langle\alpha'|Y(a)|\beta'\rangle \tag{2.3.8}$$

where $Y(a)$ is an arbitrary operator in the radiator subspace. Combining Eqs. (2.3.4) and (2.3.8) gives to second order in the radiator-electron interaction

$$M^{(2)}_{\alpha\beta,\alpha'\beta'}(\omega) = \frac{1}{\hbar^2}\int \frac{d\vec{k}}{(2\pi)^3}\int_{-\infty}^{\infty}\frac{d\Omega}{2\pi}S_o(k,\Omega)\left\{\delta_{\beta\beta'}\sum_{\gamma}\frac{\tilde{V}_{\alpha\gamma}(\vec{k})\tilde{V}_{\gamma\alpha'}(-\vec{k})}{\Delta\omega_{\gamma\beta}-\Omega+i\eta}f_\gamma f_{\alpha'}^{-1}\right.$$
$$\left.+\delta_{\alpha\alpha'}\sum_{\gamma}\frac{\tilde{V}_{\beta'\gamma}(-\vec{k})\tilde{V}_{\alpha\beta}(\vec{k})}{\Delta\omega_{\alpha\gamma}-\Omega+i\eta}-\tilde{V}_{\alpha\alpha'}(\vec{k})\tilde{V}_{\beta'\beta}(-\vec{k})\left[\frac{1}{\Delta\omega_{\alpha'\beta}-\Omega+i\eta}+\frac{f_\alpha f_{\alpha'}^{-1}}{\Delta\omega_{\alpha\beta'}-\Omega+i\eta}\right]\right\} \tag{2.3.9}$$

where the sums are over all radiator internal states $|\gamma\rangle$ and $\eta\to 0^+$ after the evaluation of the integrals. The eigenvalues of operators involving $H(a)$ are defined as

$$H(a)|\alpha\rangle = \hbar\omega_\alpha|\alpha\rangle \quad ,$$
$$\Delta\omega_{\alpha\beta} = \omega-(\omega_\alpha-\omega_\beta) \quad , \tag{2.3.10}$$
$$f_o(a)|\alpha\rangle = f_\alpha|\alpha\rangle \quad ,$$

where the density matrix diagonal nature in the energy eigenstate representation for stationary systems was used. The radiator-electron interaction matrix elements are given by

$$\tilde{V}_{\alpha\beta}(\vec{k}) = \langle\alpha|\tilde{V}(a,\vec{k})|\beta\rangle \quad ,$$
$$V(a,1) = \int\frac{d\vec{k}}{(2\pi)^3}\exp(-i\vec{k}\cdot\vec{r}_1)\tilde{V}(a,\vec{k}) \quad , \tag{2.3.11}$$

with $\vec{r}_1$ the perturbing electron position operator and $\hbar\vec{k}$ the momentum transferred to the perturbing electron during the collision.

2.4 Dynamic structure factor

The dynamic structure factor for an ideal quantum electron gas, $S_o(k,\omega)$, was introduced in Eq. (2.3.9) by using [19]

$$n_e \int \frac{d\vec{q}}{(2\pi)^3} \frac{f_o(q)}{\hbar\omega - E_o(q) + E_o(\vec{q}+\vec{k}) + i\eta} = \hbar^{-1} \int_{-\infty}^{\infty} \frac{d\Omega}{2\pi} \frac{S_o(k,\Omega)}{\omega - \Omega + i\eta} \tag{2.4.1}$$

where $f_o(q)$ are the momentum distribution and $E_o(q) = \hbar^2 q^2 / 2m$ the kinetic energy of the perturbing electron with *m* the electron mass.

In the experiments of interest the electron gas is assumed to be in local thermal equilibrium so that the dynamic structure factor satisfies the detailed-balance property [19]

$$S_o(k,-\omega) = e^{\hbar\omega/T} S_o(k,\omega) \quad \text{(LTE)}. \tag{2.4.2}$$

It expresses that to destroy an excitation of energy $\hbar\omega$ in the electron gas, it must first exist with relative abundance given by the Boltzmann factor. This asymmetry led to theoretical line shifts from electron collisions among levels with the same principle quantum number ($\Delta n = 0$) in hydrogen atoms that incorrectly vanish in a semiclassical approximation. [20]

In order to retain the detailed-balance property in the classical limit of the thermal averages, a consistent approach is required. This is accomplished by

$$S_o(k,\omega) \to S_o^{(cl)}(k,\omega) \begin{cases} 1 & \omega > 0 \\ e^{-\hbar\omega/T} & \omega < 0 \end{cases} \tag{2.4.3}$$

where

$$S_o^{(cl)}(k,\omega) = \frac{n_e}{k} \sqrt{\frac{2\pi m}{T}} \exp\left\{ -\frac{m\omega^2}{2k^2 T} \right\} \tag{2.4.4}$$

is the dynamic structure factor for an ideal classical electron gas in thermal equilibrium. [19]

2.5 Isolated lines

For isolated lines where the widths and shifts produced by the perturbing electrons are much smaller than the energy separation between adjacent radiator levels of different total angular momentum, the line shape function is approximately written as, [15,21]

$$I(\omega) = \pi^{-1} \sum_{m_\mu} \sum_{m_\nu} \left| \vec{d}_{\mu\nu} \right|^2 \left\{ f_\mu \frac{\gamma_{\mu\nu}(\omega)}{\Delta\omega_{\mu\nu}^2 + \gamma_{\mu\nu}^2(\omega)} + f_\nu \frac{\gamma_{\nu\mu}(\omega)}{\Delta\omega_{\nu\mu}^2 + \gamma_{\nu\mu}^2(\omega)} \right\} \tag{2.5.1}$$

where for clarity line shifts were neglected,

$$\vec{d}_{\alpha\beta} = \langle \alpha | \vec{d} | \beta \rangle \quad , \tag{2.5.2}$$

$$\gamma_{\alpha\beta}(\omega) = -\operatorname{Im} M_{\alpha\beta,\alpha\beta}(\omega) \quad , \tag{2.5.3}$$

and the sums are over magnetic quantum numbers. The adopted convention has upper radiator internal states designated by $|\mu\rangle$, $|\mu'\rangle$, etc and lower states by $|\nu\rangle$, $|\nu'\rangle$, etc.

2.6 Emission and absorption line profiles

The energy loss and gain by a radiation field to and from a plasma is described by the plasma emission and absorption coefficients. Thus, these coefficients relate experimental quantities to the line shape function.

The emission coefficient is given by [22]

$$\varepsilon(\omega) = n_a \frac{\omega^4}{3\pi c^3} \operatorname{Re} \int_{-\infty}^{\infty} \frac{dt}{2\pi} e^{i\omega t} \left\langle \vec{d} \cdot \vec{d}(t) \right\rangle \tag{2.6.1}$$

with c the speed of light in vacuum and n_a the radiator number density. The absorption coefficient is given by [22]

$$\kappa(\omega) = n_a \frac{4\pi^2 \omega}{3\hbar c} \operatorname{Re} \int_{-\infty}^{\infty} \frac{dt}{2\pi} e^{i\omega t} \left\{ \left\langle \vec{d}(t) \cdot \vec{d} \right\rangle - \left\langle \vec{d} \cdot \vec{d}(t) \right\rangle \right\} \tag{2.6.2}$$

where the subtracted term accounts for stimulated emission.

In local thermal equilibrium, [19]

$$\int_{-\infty}^{\infty} \frac{dt}{2\pi} e^{i\omega t} \left\langle \vec{d}(t) \cdot \vec{d} \right\rangle = e^{\hbar\omega/T} \int_{-\infty}^{\infty} \frac{dt}{2\pi} e^{i\omega t} \left\langle \vec{d} \cdot \vec{d}(t) \right\rangle \quad \text{(LTE)} \tag{2.6.3}$$

so that

$$\frac{\varepsilon(\omega)}{\kappa(\omega)} = \frac{\hbar\omega^3}{4\pi^3 c^2\left(e^{\hbar\omega/T}-1\right)} \quad \text{(LTE)} \tag{2.6.4}$$

satisfying the Kirchhoff-Planck relation. [22]

Combining Eqs. (2.2.1), (2.5.1), (2.6.1), and (2.6.2) to get the emission and absorption coefficients for $\omega > 0$ near the isolated line center, $\omega_o = \omega_\mu - \omega_\nu > 0$, yields (neglecting Doppler and ion broadening)

$$\varepsilon(\omega) = n_a \frac{\omega^4}{3\pi c^3} \sum_{m_\mu} \sum_{m_\nu} \left|\vec{d}_{\mu\nu}\right|^2 f_\mu \frac{\gamma_{\mu\nu}(\omega_o)/\pi}{(\omega-\omega_o)^2 + \gamma_{\mu\nu}^2(\omega_o)} \tag{2.6.5}$$

and

$$\kappa(\omega) = n_a \frac{4\pi^2\omega}{3\hbar c} \sum_{m_\mu} \sum_{m_\nu} \left|\vec{d}_{\mu\nu}\right|^2 \left[f_\nu \frac{\gamma_{\nu\mu}(-\omega_o)/\pi}{(\omega-\omega_o)^2 + \gamma_{\nu\mu}^2(-\omega_o)} - f_\mu \frac{\gamma_{\mu\nu}(\omega_o)/\pi}{(\omega-\omega_o)^2 + \gamma_{\mu\nu}^2(\omega_o)} \right] . \tag{2.6.6}$$

The widths were taken in the impact limit $(\Delta\omega \to 0)$ and the terms with a maximum near $\omega = -\omega_o$ were assumed negligible in the positive-frequency parts of $\varepsilon(\omega)$ and $\kappa(\omega)$. In thermal equilibrium the Kirchhoff-Planck relation requires $\gamma_{\mu\nu}(\omega_o) = \gamma_{\nu\mu}(-\omega_o)$. For radiator level populations in stationary non-equilibrium, however, $\gamma_{\mu\nu}(\omega_o) \neq \gamma_{\nu\mu}(-\omega_o)$ as shown below.

3. TWO-LEVEL RADIATOR

To illustrate the present results, the second-order expression for the width is applied to the isolated lines of a two-level radiator, each with possible rotational degeneracy. Furthermore, the assumed radiator-electron interaction, appropriate for a Li-like system, describes a radiator with one bound electron outside a frozen, spherically symmetric core,

$$\tilde{V}\left(a,\vec{k}\right) = \frac{4\pi e^2}{k^2}\left[e^{i\vec{k}\cdot\vec{r}_a} - 1\right] \tag{3.1}$$

with e the electron electric charge and $\vec{r}_a$ the bound electron position operator. Results for a multi-level radiator are briefly discussed in *Appendix A*.

It is advantageous to separate the width contributions according to the kind of collision,

$$\gamma_{\alpha\beta}(\omega) = \gamma_{\alpha\beta}^{in}(\omega) + \gamma_{\alpha\beta}^{el}(\omega) \tag{3.2}$$

where *in* and *el* denote inelastic and elastic radiator-electron collisions, respectively.

The second-order inelastic collision contribution to the width includes interaction terms involving the upper and lower radiator internal states (e.g.; $\tilde{V}_{\mu\nu}$), but not those involving only the upper or only the lower states (e.g.; $\tilde{V}_{\mu\mu'}$ or $\tilde{V}_{\nu\nu'}$). Thus, from Eqs. (2.3.9) and (2.5.3) one gets

$$\begin{Bmatrix} \gamma_{\mu\nu}^{in}(\omega) \\ \gamma_{\nu\mu}^{in}(\omega) \end{Bmatrix} = \begin{Bmatrix} f_\nu f_\mu^{-1} \\ 1 \end{Bmatrix} \left\langle \sigma_\mu^{in}(\omega) \right\rangle + \begin{Bmatrix} 1 \\ f_\mu f_\nu^{-1} \end{Bmatrix} \left\langle \sigma_\nu^{in}(\omega) \right\rangle \tag{3.3}$$

where

$$\begin{Bmatrix} \left\langle \sigma_\mu^{in}(\omega) \right\rangle \\ \left\langle \sigma_\nu^{in}(\omega) \right\rangle \end{Bmatrix} = \frac{1}{2\hbar^2} \int \frac{d\vec{k}}{(2\pi)^3} S_o(k,\omega) \begin{Bmatrix} \sum_{m_{\nu'}} \left| \tilde{V}_{\mu\nu'}\left(\vec{k}\right) \right|^2 \\ \sum_{m_{\mu'}} \left| \tilde{V}_{\mu'\nu}\left(\vec{k}\right) \right|^2 \end{Bmatrix} \quad . \tag{3.4}$$

Inserting the interaction in Eq. (3.1), neglecting spin, and performing the angular integrations as well as the sums over magnetic quantum numbers yields

$$\begin{Bmatrix} \left\langle \sigma_\mu^{in}(\omega) \right\rangle \\ \left\langle \sigma_\nu^{in}(\omega) \right\rangle \end{Bmatrix} = \begin{Bmatrix} (2\ell_\nu + 1) \\ (2\ell_\mu + 1) \end{Bmatrix} \int_o^\infty dk\, S_o(k,\omega) \sum_{\ell=0}^\infty (2\ell+1) \left[J_{\mu\nu}^{(\ell)}(k) \right]^2 \quad , \tag{3.5}$$

$$J_{\mu\nu}^{(\ell)}(k) = \frac{2e^2}{\hbar k} \begin{pmatrix} \ell_\mu & \ell & \ell_\nu \\ 0 & 0 & 0 \end{pmatrix} \int_o^\infty dr\, r^2 j_\ell(kr) R_\mu(r) R_\nu(r) \quad , \tag{3.6}$$

with $R_\alpha(r)$ and ℓ_α the radial wavefunction and orbital quantum number for the radiator state $|\alpha\rangle$, respectively, and $j_\ell(x)$ the spherical Bessel function of order ℓ. [23] It follows that

$$\left(2\ell_{\mu}+1\right)\left\langle\sigma_{\mu}^{in}(\omega)\right\rangle=\left(2\ell_{\nu}+1\right)\left\langle\sigma_{\nu}^{in}(\omega)\right\rangle \quad . \tag{3.7}$$

Note that the inelastic collision width contributions in Eq. (3.3) depend on the population of the radiator internal states, terms that are absent in the standard impact theory. [15]

The second-order elastic collision contribution to the line width includes terms with $\tilde{V}_{\mu\mu'}$ and $\tilde{V}_{\nu\nu'}$ but not those containing $\tilde{V}_{\mu\nu}$. Thus, after straightforward manipulations Eq. (2.3.9) gives

$$\begin{Bmatrix}\gamma_{\mu\nu}^{el}(\omega)\\ \\ \gamma_{\nu\mu}^{el}(\omega)\end{Bmatrix}=\begin{Bmatrix}\left\langle F_{\mu\nu}(\omega)\right\rangle\\ \\ \left\langle F_{\nu\mu}(\omega)\right\rangle\end{Bmatrix} \tag{3.8}$$

where

$$\left\langle F_{\alpha\beta}(\omega)\right\rangle=\frac{1}{2\hbar^{2}}\int\frac{d\vec{k}}{(2\pi)^{3}}S_{o}\left(k,\Delta\omega_{\alpha\beta}\right)\left|\tilde{V}_{\alpha\alpha}\left(\vec{k}\right)-\tilde{V}_{\beta\beta}\left(-\vec{k}\right)\right|^{2} \quad . \tag{3.9}$$

The dependence on the radiator level populations cancels in the elastic contribution since f_{α} is assumed independent of magnetic quantum numbers.

For an LTE electron gas the absorption and emission width contributions are then related by

$$\gamma_{\nu\mu}^{in}(-\omega)=f_{\mu}f_{\nu}^{-1}e^{\hbar\omega/T}\gamma_{\mu\nu}^{in}(\omega) \tag{3.10}$$

and

$$\gamma_{\nu\mu}^{el}(-\omega)=e^{\hbar\Delta\omega_{\mu\nu}/T}\gamma_{\mu\nu}^{el}(\omega) \tag{3.11}$$

which follow from the detailed-balance property of the dynamic structure factor. From Eqs. (3.10) and (3.11) one obtains in the impact limit $\left(\Delta\omega\rightarrow 0\right)$

$$\gamma_{\nu\mu}(-\omega_{o})=\gamma_{\mu\nu}(\omega_{o})+\left(P_{\mu\nu}-1\right)\gamma_{\mu\nu}^{in}(\omega_{o}) \tag{3.12}$$

with

$$P_{\mu\nu}=f_{\mu}f_{\nu}^{-1}e^{\hbar\left(\omega_{\mu}-\omega_{\nu}\right)/T} \tag{3.13}$$

In thermal equilibrium $P_{\mu\nu}=1$ and $\gamma_{\nu\mu}(-\omega_o)=\gamma_{\mu\nu}(\omega_o)$ satisfying the Kirchhoff-Planck relation.

4. COMPARISON TO STANDARD IMPACT THEORY

The standard impact theory [15] uses a Maxwellian velocity distribution to describe the electron gas, which seems appropriate for the relatively high experimental temperatures. [1-9] A comparison of the kinetic and standard impact theories then requires the classical limit of the thermally averaged collision cross-sections.

For a classical electron gas in LTE the emission and absorption line widths are obtained using Eq. (2.4.3) so that

$$\begin{Bmatrix}\gamma_{\mu\nu}(\omega_o)\\ \\ \gamma_{\nu\mu}(-\omega_o)\end{Bmatrix}\rightarrow\begin{Bmatrix}\gamma^{cl}_{\mu\nu}(\omega_o)\\ \\ \gamma^{cl}_{\nu\mu}(-\omega_o)\end{Bmatrix}=\begin{Bmatrix}P_{\nu\mu}\\ \\ 1\end{Bmatrix}e^{\hbar\omega_o/T}\left\langle\sigma^{in}_{\mu}(\omega_o)\right\rangle_{cl}+\begin{Bmatrix}1\\ \\ P_{\mu\nu}\end{Bmatrix}\left\langle\sigma^{in}_{\nu}(\omega_o)\right\rangle_{cl}+\left\langle F_{\mu\nu}(\omega_o)\right\rangle_{cl}\qquad(4.1)$$

where $\langle\cdots\rangle_{cl}$ denotes the thermal average in Eqs. (3.4) and (3.9) but with the classical ideal gas dynamic structure factor in Eq. (2.4.4). Clearly, $\gamma^{cl}_{\nu\mu}(-\omega_o)\neq\gamma^{cl}_{\mu\nu}(\omega_o)$ except for LTE radiator level populations as required by the Kirchhoff-Planck relation. [22]

As shown in *Appendix B* the second-order width in the standard electron impact theory [15] is given by

$$\gamma_{std}(\omega_o)=\left\langle\sigma^{in}_{\mu}(\omega_o)\right\rangle_{cl}+\left\langle\sigma^{in}_{\nu}(\omega_o)\right\rangle_{cl}+\left\langle F_{\mu\nu}(\omega_o)\right\rangle_{cl}\quad.\qquad(4.2)$$

Note that $S^{(cl)}_o(k,\omega)$ in $\langle\cdots\rangle_{cl}$ is symmetric in ω and does not satisfy the detailed-balance condition. Hence, $\gamma_{std}(\omega_o)=\gamma_{std}(-\omega_o)$ giving identical emission and absorption profiles independent of the radiator level populations.

The comparison of the isolated line width expressions for a two-level radiator from kinetic theory in Eq. (4.1) and the standard impact theory in Eq. (4.2) is the main result of the paper. The former displays radiator internal state population dependent corrections due to retaining initial

correlations until the end of the formal development as well as corrections due to the detailed-balance property of the electron gas.

5. EXPERIMENTAL DISCUSSION

To motivate an experimental resolution of the width discrepancies, [1-13] the results in Sect. 4 are applied to previous as well as proposed isolated line width experiments. For convenience the discussion treats the Li-like *2p-2s* and *3p-3s* lines separately.

5.1 BIII *2p-2s* lines

The two-level radiator is an excellent approximation to the BIII *2p-2s* lines since the upper and lower levels in the transition are well isolated from all other radiator states. [10] These lines have $\hbar\omega_o \approx 6eV$ and the experimental conditions were $n_e = 1.81\times10^{18}$ cm^{-3} and $T = 10.6eV$. [3] At the experimental conditions close-coupling calculations [10] yield standard impact widths that are about half the experimental results. In addition, the contribution to the width from inelastic collisions is about twice that from elastic collisions. [10]

Assuming that the second-order results extend to the all-order formulation, one gets using Eqs. (3.2) and (4.2)

$$\left\langle F_{\mu\nu}(\omega_o)\right\rangle_{cl} \approx \gamma^{el}_{std} \tag{5.1.1}$$

and

$$\gamma^{in}_{std}(\omega_o) = \left\langle \sigma^{in}_{\mu}(\omega_o)\right\rangle_{cl} + \left\langle \sigma^{in}_{\nu}(\omega_o)\right\rangle_{cl} \approx 2\gamma^{el}_{std} \quad . \tag{5.1.2}$$

Then Eq. (3.7) and Eq. (5.1.2) give

$$\left\langle \sigma^{in}_{\mu}(\omega_o)\right\rangle_{cl} \approx \gamma^{el}_{std}/2 \quad , \tag{5.1.3}$$

$$\left\langle \sigma^{in}_{\nu}(\omega_o)\right\rangle_{cl} \approx 3\gamma^{el}_{std}/2 \quad , \tag{5.1.4}$$

with $\ell_{\mu} = 1$ and $\ell_{\nu} = 0$ corresponding to the *2p-2s* line.

If the experiments were in thermal equilibrium, then at the experimental conditions [3] Eqs. (5.1.1) through (5.1.4) together with Eqs. (4.1) and (4.2) yield

$$\gamma^{cl}_{\mu\nu}(\omega_o) = \gamma^{cl}_{\nu\mu}(-\omega_o) \approx 1.1\gamma_{std}(\omega_o) \quad \text{(LTE)} \tag{5.1.5}$$

only slightly improving agreement with the experimental width. The radiator level populations in the experiments, however, were not in thermal equilibrium with the electron gas. [24] Unfortunately, there are no estimates of the ratio $f_\nu f_\mu^{-1}$ to test the kinetic theory results and a population kinetics simulation is beyond the scope of the present work.

Interestingly, the radiator level populations were briefly discussed in Ref. 10 where the absence of the BIII *4f-3d* line was used to argue for a lower experimental temperature. Applying this interpretation to the bound electrons (not the perturbing electron gas which is well-characterized by Thomson scattering [3]), then the BIII level populations could be described by an effective LTE temperature of say 4 eV. [10] The resulting ratio of $f_\nu f_\mu^{-1} = 4.5$ substituted into Eq. (4.1) and again using Eqs. (5.1.1) through (5.1.4) yields for the emission width

$$\frac{\gamma^{cl}_{\mu\nu}(\omega_o)}{\gamma_{std}(\omega_o)} = 1.6 \quad \text{(Non-LTE).} \tag{5.1.6}$$

Accounting for the ion quadrupole width contribution of ~10%, [10] the experimental and kinetic theory emission widths now disagree by 16%, not far outside the $\pm 10\%$ experimental error. [3] Of course, the assumed LTE distribution with a 4 eV effective temperature is only a plausible choice, but shows that the width corrections from the kinetic theory method can be significant.

5.2 Proposed experiments

The results above suggest possible experiments to test electron impact theories of isolated lines. The idea is to repeat the experiments [1-9] with the additional measurement of the

absorption coefficient. If the initial and final radiator level populations are in LTE, then the emission and absorption profiles are identical. Thus, (neglecting Doppler and ion broadening)

$$\left.\begin{matrix}\varepsilon(\omega)\\ \kappa(\omega)\end{matrix}\right\} \propto \frac{\gamma_{\mu\nu}(\omega_o)}{(\omega-\omega_o)^2+\gamma_{\mu\nu}^2(\omega_{o.})} \quad \text{(LTE).} \tag{5.2.1}$$

As noted earlier, however, experiments typically have non-LTE radiator level populations.

Contrary to the standard impact theory, [15] for stationary non-equilibrium radiator populations the kinetic theory method predicts different emission and absorption widths. Therefore, (neglecting Doppler and ion broadening)

$$\left.\begin{matrix}\varepsilon(\omega)\\ \kappa(\omega)\end{matrix}\right\} \propto \begin{cases} \dfrac{\gamma_{\mu\nu}(\omega_o)}{(\omega-\omega_o)^2+\gamma_{\mu\nu}^2(\omega_o)} \\ \dfrac{f_\nu\gamma_{\nu\mu}(-\omega_o)}{(\omega-\omega_o)^2+\gamma_{\nu\mu}^2(-\omega_{o.})} - \dfrac{f_\mu\gamma_{\mu\nu}(\omega_o)}{(\omega-\omega_o)^2+\gamma_{\mu\nu}^2(\omega_o)} \end{cases} \quad \text{(Non-LTE).} \tag{5.2.2}$$

The proposal exploits the difference between $\varepsilon(\omega)$ and $\kappa(\omega)$ in Eq. (5.2.2).

Applying the same ratio of $f_\nu f_\mu^{-1} = 4.5$ in the emission analysis to the BIII *2p-2s* absorption line width at the experimental conditions [3] yields

$$\frac{\gamma_{\mu\nu}^{cl}(\omega_o)}{\gamma_{\nu\mu}^{cl}(-\omega_o)} \approx 1.9 \quad \text{(Non-LTE).} \tag{5.2.3}$$

This leads to different frequency dependence in the emission and absorption coefficients that should be discernible by experiments as shown in Fig. 1.

Figure 1 displays $\varepsilon(\omega)$ and $\kappa(\omega)$ from Eq. (5.2.2). The widths calculations assumed $f_\nu f_\mu^{-1} = 4.5$ with $\gamma_{std}(\omega_o) = 0.055$ Å. [10] To check the plausibility of measuring the difference; both Doppler and instrumental broadening [3] were included in generating the results in Fig. 1.

In obtaining the absorption coefficient it was assumed that the isolated lines were optically thin so that the transmission, $T(\omega)$, is given by

$$T(\omega) - 1 = e^{-\tau(\omega)} - 1 \approx \tau(\omega) \propto \kappa(\omega) \tag{5.2.4}$$

with $\tau(\omega)$ the sample optical depth. Therefore, instrumental broadening is equivalent for $T(\omega)$ and $\kappa(\omega)$. Although complete verification of the present results requires experimental determination of the ratio $f_\nu f_\mu^{-1}$, different experimental $\varepsilon(\omega)$ and $\kappa(\omega)$ profiles would substantiate them and challenge the standard impact theory [15] for isolated lines.

5.3 The Li-like *3p-3s* isoelectronic sequence

A feature of the *3p-3s* isolated lines is the monotonic increase in disagreement along the Li-like isoelectronic sequence between theory and experiments. [2-6,8-13] This observation was puzzling since the electron standard impact widths for isolated lines of multiply charged ions is dominated by inelastic collisions. [11-13] This is a process for which the convergent close-coupling method used in the width calculations is considered highly accurate. This trend is displayed in Fig. 2 where the ratios of experimental to theoretical widths are plotted as a function of nuclear charge. The experimental values for Fig. 2 are the average of the *3p-3s* doublet lines at each plasma condition. [2,6,9] The theoretical widths are obtained by interpolating quantum-mechanical calculations [13] using standard impact theory.

Although the two-level radiator is more appropriate for the Li-like *2p-2s* transitions than the *3p-3s* transitions, the general result also applies to these isolated lines. That is, there is dependence on the non-LTE radiator level populations in the inelastic collision contribution to the width absent in the standard impact theory [15] (see *Appendix A*).

The conditions for LTE can be estimated from a simple formula derived for steady-state plasmas [25]

$$n_e^* \geq \frac{7\times10^{18} Z_{eff}^6}{n^{17/2}} \frac{T}{E_H} \left[cm^{-3}\right] \qquad (5.3.1)$$

where n_e^* is the minimum electron density required for principle quantum number n to be in LTE with the perturbing electron gas, E_H is the ionization energy of the hydrogen atom ground state, and Z_{eff} the effective hydrogenic charge.

The ratios n_e^*/n_e for the various experiments [2,6,9] are plotted in Fig. 3 indicating that in most cases non-LTE populations are expected for the $n = 3$ levels. Furthermore, in each set of experiments the $n = 3$ level populations are increasingly further away from LTE conditions with increasing atomic number. It follows from Eq. (4.1) that the correction to the emission width increases as the ratio of the upper to lower radiator state populations decreases. Consequently, the level population dependence of the isolated line widths may explain the increasing discrepancy along the isoelectronic sequence.

The present results may also explain some of the scatter in the experimental data (see Fig. 2). Since line shapes for a given element are measured over a range of plasma conditions, the radiator internal steady-state populations can significantly vary affecting the line widths. A consequence of this interpretation is to introduce uncertainty into past measurements [1-9] through the width dependence on level populations. Future experiments can attempt to reach thermal equilibrium or measure the level populations. Otherwise, comparisons with theory may have to rely on kinetic population models.

6. CONCLUSION

A possible explanation of the existing discrepancies [1-13] between experimental and theoretical widths of isolated lines was presented. The corrections are due to neglected initial correlations and incomplete treatment of the classical electron gas in the standard impact theory.

[15] For isolated lines these approximations introduce significant errors so that a more complete theory is required.

The second-order kinetic theory results [16] were extended to stationary non-equilibrium states. It was shown that the Rydberg-Ritz principle [26] does not apply to isolated lines involving non-LTE level populations. That is, the line profile is not described by the addition of independent level widths (e.g.; the sum of thermally averaged inelastic cross-sections), but rather a line width that explicitly depends on the pair of initial and final levels through their steady-state populations. Furthermore, a consistent classical limit of the quantum electron gas introduces corrections to the width. Both corrections are essential in satisfying the Kirchhoff-Planck relation. In second-order theory the corrections enter as multiplicative factors to the thermally averaged inelastic cross-sections allowing for width estimates based on standard impact theory (see *Appendix A*).

A repeat of earlier experiments [1-9] measuring both photon emission and absorption in the spectral region of the isolated line was proposed. Differences in the energy dependence of the emission and absorption coefficients would substantiate the present results, which predict different emission and absorption isolated line profiles for stationary non-equilibrium internal radiator states. On the other hand, the standard impact theory satisfies the Kirchhoff-Planck relation but only as a result of compensating approximations and predicts identical emission and absorption line widths independent of the radiator level population distribution.

The proposed resolution of the discrepancies relies on several approximations. The main assumptions are an ideal electron gas and a second-order expansion of the width operator. It is well known [16,17] that the main effect of the plasma interactions is to screen the radiator-electron interaction and should not significantly affect the conclusions. The good agreement

between the Coulomb-Born and R-matrix calculations for the BIII *2s-2p* line [10] suggests that using second-order theory to estimate the width corrections is reasonable, at least for that case.

Finally, the corrections to the widths can be significant for isolated lines, but are negligible for many other lines. Firstly, the radiator level population corrections to the line widths vanish for systems in thermal equilibrium. Secondly, widths are not significantly affected if the broadening due to interactions with states distant in energy from the initial and final levels is small. For example, for hydrogenic radiators the no quenching approximation [21,25] is often valid and the present corrections practically vanish.

Acknowledgements – It is a pleasure to acknowledge valuable discussions with Richard W. Lee. Work performed under the auspices of the Department of Energy by University of California, Lawrence Livermore National Laboratory under Contract W-7405-ENG-48.

APPENDIX A: MULTI-LEVEL RADIATOR

This Appendix extends the second-order kinetic theory emission and absorption widths of isolated lines from a two-level to a multi-level radiator. The elastic collision contributions to the widths remain unchanged. The inelastic collision contributions, however, are modified.

Define the thermally averaged inelastic collision cross-section from a state $|\alpha\rangle$ with total angular momentum J_α to all $(2J_\beta+1)$ states of a level with total angular momentum J_β as

$$\left\langle \sigma^{in}_{\alpha\to\beta}(\omega_o)\right\rangle = \frac{1}{2\hbar^2}\int \frac{d\vec{k}}{(2\pi)^3} S_o\left(k,\omega_\alpha-\omega_\beta\right)\sum_{m_\beta}\left|\tilde{V}_{\alpha\beta}\left(\vec{k}\right)\right|^2 \tag{A1}$$

The identification of the expression in Eq. (A1) with a thermally averaged collision cross-section is provided in *Appendix B*. Then, using Eqs. (2.3.9) and (2.5.3) the second-order inelastic impact emission and absorption widths for an electron gas in LTE can be written as

$$\begin{Bmatrix} \gamma^{in}_{\mu\nu}(\omega_o) \\ \gamma^{in}_{\nu\mu}(-\omega_o)\end{Bmatrix} = \sum_{J_\alpha\neq J_\mu}\begin{Bmatrix} f_\alpha f_\mu^{-1} \\ e^{\hbar(\omega_\mu-\omega_\alpha)/T}\end{Bmatrix}\left\langle \sigma^{in}_{\mu\to\alpha}(\omega_o)\right\rangle + \sum_{J_\alpha\neq J_\nu}\begin{Bmatrix} e^{\hbar(\omega_\nu-\omega_\alpha)/T} \\ f_\alpha f_\nu^{-1}\end{Bmatrix}\left\langle \sigma^{in}_{\nu\to\alpha}(\omega_o)\right\rangle \quad . \tag{A2}$$

To make contact with the standard impact theory, [15] take the classical limit of the electron gas. Then, using Eq. (2.4.3) one gets

$$\begin{Bmatrix} \gamma^{in}_{\mu\nu}(\omega_o) \\ \gamma^{in}_{\nu\mu}(-\omega_o)\end{Bmatrix} \to \sum_{J_\alpha\neq J_\mu}\left[e^{\hbar(\omega_\mu-\omega_\alpha)/T}\theta(\omega_\mu-\omega_\alpha)+\theta(\omega_\alpha-\omega_\mu)\right]\begin{Bmatrix} P_{\alpha\mu} \\ 1\end{Bmatrix}\left\langle \sigma^{in}_{\mu\to\alpha}(\omega_o)\right\rangle_{cl}$$

$$+\sum_{J_\alpha\neq J_\nu}\left[e^{\hbar(\omega_\nu-\omega_\alpha)/T}\theta(\omega_\nu-\omega_\alpha)+\theta(\omega_\alpha-\omega_\nu)\right]\begin{Bmatrix} 1 \\ P_{\alpha\nu}\end{Bmatrix}\left\langle \sigma^{in}_{\nu\to\alpha}(\omega_o)\right\rangle_{cl} \tag{A3}$$

where

$$\theta(x) = \begin{cases} 1 & x \geq 0 \\ 0 & x < 0 \end{cases} \quad . \tag{A4}$$

The brackets $[\cdots]$ in Eq. (A3) display the detailed-balance property of the electron gas asserting that electron impact de-excitations are more probable by a Boltzmann factor than excitations.

The brackets $\{\cdots\}$ in Eq. (A3) contain the level population corrections. These corrections depend on the deviations from thermal equilibrium. That is,

$$P_{\alpha\beta} = f_\alpha f_\beta^{-1} e^{\hbar(\omega_\alpha - \omega_\beta)} \xrightarrow[LTE]{} 1 \tag{A5}$$

and $\gamma_{\nu\mu}(-\omega_o) = \gamma_{\mu\nu}(\omega_o)$ satisfying the Kirchhoff-Planck relation. [22] Furthermore, the population dependent corrections are present only for electron inelastic collisions involving the initial states of the isolated line.

Equation (A3), in conjunction with thermally averaged inelastic cross-sections from standard impact theory [15] and level populations from kinetic steady-state models, provides a basis for numerical comparisons of theory and experiment.

APPENDIX B: PROOF OF EQUATION (4.2)

This Appendix shows that the expression for $\gamma_{std}(\omega_o)$ in Eq. (4.2) is identical to the second-order standard impact theory. [15] To proceed, write the dynamic structure factor for an ideal classical electron gas in the form [19]

$$S_o^{(cl)}(k,\omega) = \frac{n_e}{2}\int_o^\infty du\, F(u)\int d\Omega_{\hat{u}}\,\delta\left(\omega - \vec{k}\cdot\vec{u}\right) \tag{B1}$$

where $d\Omega$ are the differential solid angle and $F(u)$ the Maxwellian velocity distribution with normalization

$$\int_o^\infty du F(u) = 1 \quad . \tag{B2}$$

Using Eq. (B1) write the inelastic contributions to the upper level width as

$$\begin{aligned}
\left\langle \sigma_\mu^{in}(\omega_o)\right\rangle_{cl} &= \frac{n_e}{4\hbar^2}\int \frac{d\vec{k}}{(2\pi)^3}\int_o^\infty du\, F(u)\int d\Omega_{\hat{u}}\;\delta\left(\omega_o - \vec{k}\cdot\vec{u}\right)\sum_{m_v}\left|\tilde{V}_{\mu v}\left(\vec{k}\right)\right|^2 \\
&= \frac{n_e}{(4\pi\hbar)^2}\int_o^\infty \frac{du}{u}F(u)\int d\Omega_{\hat{u}}\sum_{m_v}\left|\tilde{V}_{\mu v}\left(\vec{k}\right)\right|^2\int_{k_1}^{k_2} dk\,k \\
&= \frac{n_e}{2}\int_o^\infty du\, uF(u)\int d\Omega_{\hat{u}}\,\frac{k_f}{k_i}\sum_{m_v}\left|\frac{m}{2\pi\hbar^2}\tilde{V}_{\mu v}(\vec{u})\right|^2 \\
&= \frac{n_e}{2}\int_o^\infty du\, uF(u)\sigma_\mu^{in} \quad .
\end{aligned} \tag{B3}$$

The k-integration limits are determined from momentum and energy conservation,

$$\vec{k} = \vec{k}_f - \vec{k}_i \quad , \tag{B4}$$

$$\frac{\hbar^2 k_i^2}{2m} = \frac{m u^2}{2} \quad , \qquad \text{and} \qquad \frac{\hbar^2 k_f^2}{2m} = \frac{\hbar^2 k_i^2}{2m} + \hbar\omega_o \quad , \tag{B5}$$

where $\hbar k_i$ and $\hbar k_f$ are the initial and final momentum of the perturbing electron, respectively. Hence, in the second line of Eq. (B3)

$$k_1^2 = k_i^2 + k_f^2 - 2k_i k_f \qquad \text{and} \qquad k_2^2 = k_i^2 + k_f^2 + 2k_i k_f \quad . \tag{B6}$$

The inelastic cross-section in the Born approximation is given by [27]

$$\sigma_\mu^{in} = \int d\Omega \frac{d\sigma_\mu^{in}}{d\Omega} = \int d\Omega \frac{k_f}{k_i} \sum_{m_\nu} \left| \frac{m}{2\pi\hbar^2} \tilde{V}_{\mu\nu}(\vec{u}) \right|^2 \tag{B7}$$

which was used to get the last line of Eq. (B3). Similar manipulations lead to

$$\left\langle \sigma_\nu^{in}(\omega_o) \right\rangle_{cl} = \frac{n_e}{2} \int_o^\infty du\, u F(u) \sigma_\nu^{in} \quad . \tag{B8}$$

Again using Eq. (B1) the elastic contributions is written as

$$\begin{aligned} \left\langle F_{\mu\nu}(\omega_o) \right\rangle_{cl} &= \frac{n_e}{4\hbar^2} \int \frac{d\vec{k}}{(2\pi)^3} \int_o^\infty du\, F(u) \int d\Omega_{\hat{u}}\, \delta(\vec{k} \cdot \vec{u}) \left| \tilde{V}_{\mu\mu}(\vec{k}) - \tilde{V}_{\nu\nu}^*(\vec{k}) \right|^2 \\ &= \frac{n_e}{(4\pi\hbar)^2} \int_o^\infty \frac{du}{u} F(u) \int d\Omega_{\hat{u}} \left| \tilde{V}_{\mu\mu}(\vec{k}) - \tilde{V}_{\nu\nu}^*(\vec{k}) \right|^2 \int_o^{2mu/\hbar} dk\, k \\ &= \frac{n_e}{2} \int_o^\infty du\, u F(u) \int d\Omega_{\hat{u}} \left| f_\mu(\vec{u}) - f_\nu^*(\vec{u}) \right|^2 \end{aligned} \tag{B9}$$

where * denotes complex conjugate. The Born scattering amplitude is given by [27]

$$f_\alpha(\vec{u}) = -\frac{m}{2\pi\hbar^2} \tilde{V}_{\alpha\alpha}(\vec{u}) \quad , \tag{B10}$$

which was used in obtaining the last line of Eq. (B9).

Combining results yields

$$\gamma_{std}(\omega_o) = \frac{n_e}{2} \int_o^\infty du\, u F(u) \left\{ \sigma_\mu^{in} + \sigma_\nu^{in} + \int d\Omega_{\hat{u}} \left| f_\mu(\vec{u}) - f_\nu^*(\vec{u}) \right|^2 \right\} \tag{B11}$$

reproducing the standard impact result for isolated lines. [15]

REFERENCES

[1] A. Sanchez, M. Blaha, & W. Jones, *Phys.Rev.* **A8**, 774(1973)

[2] S. Glenzer, N.I. Uzelac, & H.-J. Kunze, *Phys.Rev.* A45, 8795(1992)

[3] S. Glenzer & H.-J. Kunze, *Phys.Rev*. **A53**, 2225(1996)

[4] Th. Wrubel, I. Ahmad, S. Büscher, H.-J. Kunze, & S. Glenzer, *Phys.Rev.* **E57**, 5972(1998)

[5] H. Hegazy, S. Seidel, Th. Wrubel, & H.-J. Kunze, *J.Quant.Spectrosc.Radiat.Transfer* **81**, 221 (2003)

[6] S. Glenzer, N.I. Uzelac, & H.-J. Kunze, *Proceeding of the Seventh International Conference on Spectral Line Shapes* (Nova Science Publishers, New York,1993)

[7] D. Hadziomerspahic, M. Platisa, N. Konjevic, & M. Popovic, *Z.Physik* **262**, 169(1973)

[8] N. Konjevic, *Phys.Reports* **316**, 339(1999)

[9] B. Blagojevic, M.V. Popovic, N. Konjevic, & M.S. Dimitrijevic, *J.Quant.Spectrosc.Radiat.Transfer* **61**, 361(1999)

[10] H.R. Griem, Yu.V.Ralchenko & I. Bray, *Phys.Rev* **E56**, 7186(1997)

[11] Yu.V.Ralchenko, H.R. Griem, I. Bray, & D.V. Fursa, *J.Quant.Spectrosc.Radiat.Transfer* **71**, 595(2001); *Phys.Rev.* **A59**, 1890(1999)

[12] H.R. Griem, & Yu.V.Ralchenko, *J.Quant.Spectrosc.Radiat.Transfer* **65**, 287(2000)

[13] Yu.V.Ralchenko, H.R. Griem &, I. Bray *J.Quant.Spectrosc.Radiat.Transfer* **81**, 371 (2003).

[14] S. Alexiou & R.W. Lee, *Proceedings of the 15th International Conference on Spectral Line Shapes* (New York, AIP Press, 2001); *J. Quant.Spectrosc.Radiat.Transfer* (in press)

[15] M. Baranger, *Phys.Rev.* **111**, 481(1958); *ibid.* **111**, 494(1958); *ibid.* **112**, 855(1958)

[16] T. Hussey, J. Dufty, & C. Hooper, *Phys. Rev*. **A12**, 1084(1975); *ibid.* **16**, 1248(1977)

[17] J.W. Dufty & D.B. Boercker, *J.Quant.Spectrosc.Radiat.Transfer* **16**, 1065(1976)

[18] This result can be obtained by combining the transform of Eq. (2.12) with Eqs. (2.23) and (A1) of Ref. 16. Note the minor difference in the definition of the Liouville operator here and that in Ref. 16.

[19] A.G. Sitenko, *Electromagnetic Fluctuations in Plasma* (Academic Press, New York, 1976)

[20] D.B. Boercker & C.A. Iglesias, *Phys.Rev.* **A30**, 2771 (1984); H.R. Griem, C.A. Iglesias, & D.B. Boercker, *Phys.Rev.* **A44**, 5318 (1991)

[21] H.R. Griem, *Spectral Line Broadening by Plasmas* (Academic, New York, 1974)

[22] D. Mihalas, *Stellar Atmospheres* (Freeman and Co, San Francisco, 1978)

[23] M. Abramowitz & I.A. Stegun, *Handbook of Mathematical Functions* (NBS 1972)

[24] S. Glenzer, *private communication*

[25] H.R. Griem, *Plasma Spectroscopy* (McGraw-Hill, New York, 1964)

[26] U. Fano, *Phys.Rev*. **131**, 259(1963)

[27] J.R. Taylor, *Scattering Theory* (Wiley, New York, 1972)

FIGURE CAPTIONS

Fig. 1 Emission and absorption coefficients in the spectral region of the BIII *2p-2s* doublet lines. The profiles have been area normalized and include Doppler broadening. Also included is instrumental broadening described by a Voigt function with 0.071 Å Lorenztian FWHM and 0.049 Å Gaussian FWHM. [3]

Fig. 2 Ratios of experimental and theoretical *3p-3s* widths along the Li-like isoelectronic sequence: Bochum group [2,6] (*solid circles*); Belgrade group [9] (*open circles*).

Fig. 3 Ratios of the minimum electron density for principle quantum number $n = 3$ levels to reach LTE and the experimental electron density: Bochum group [2,6] (*solid circles*); Belgrade group [9] (*open circles*).

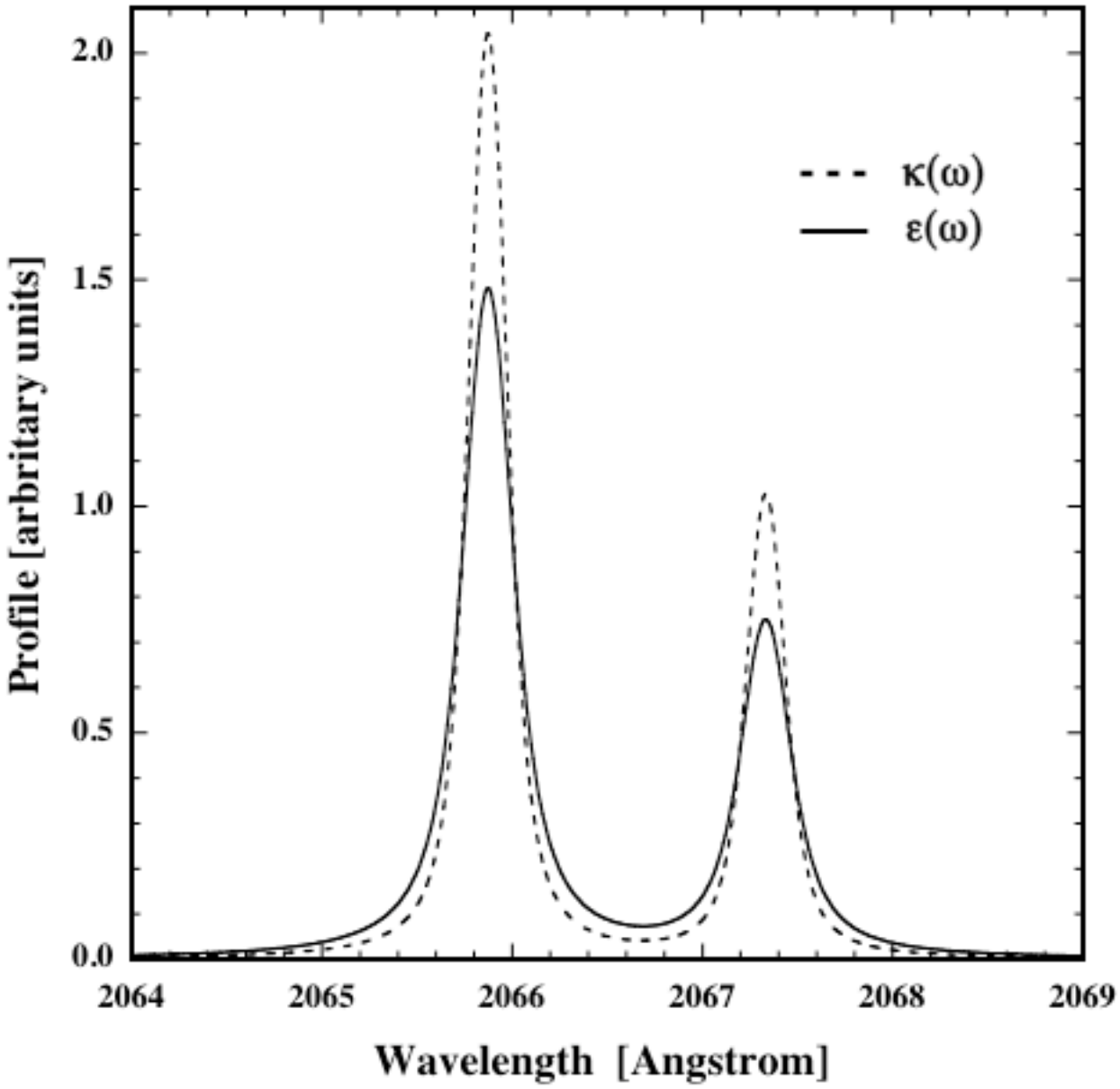
κ(ω)
ε(ω)
Profile [arbitary units]
Wavelength [Angstrom]
0.0
0.5
1.0
1.5
2.0
2064
2065
2066
2067
2068
2069

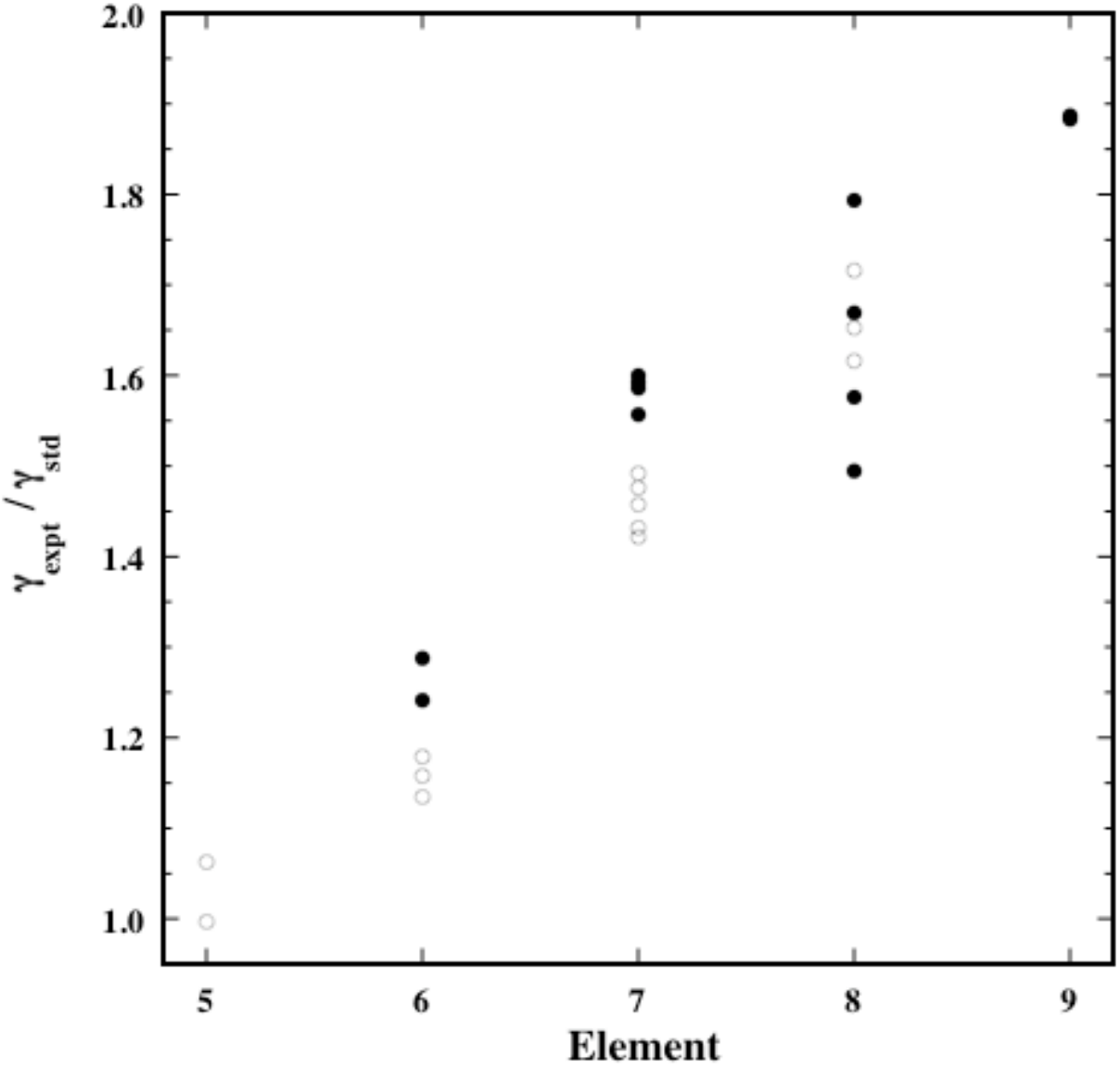
2.0
1.8
1.6
1.4
1.2
1.0
$\gamma_{expt} / \gamma_{std}$
5
6
7
8
9
Element

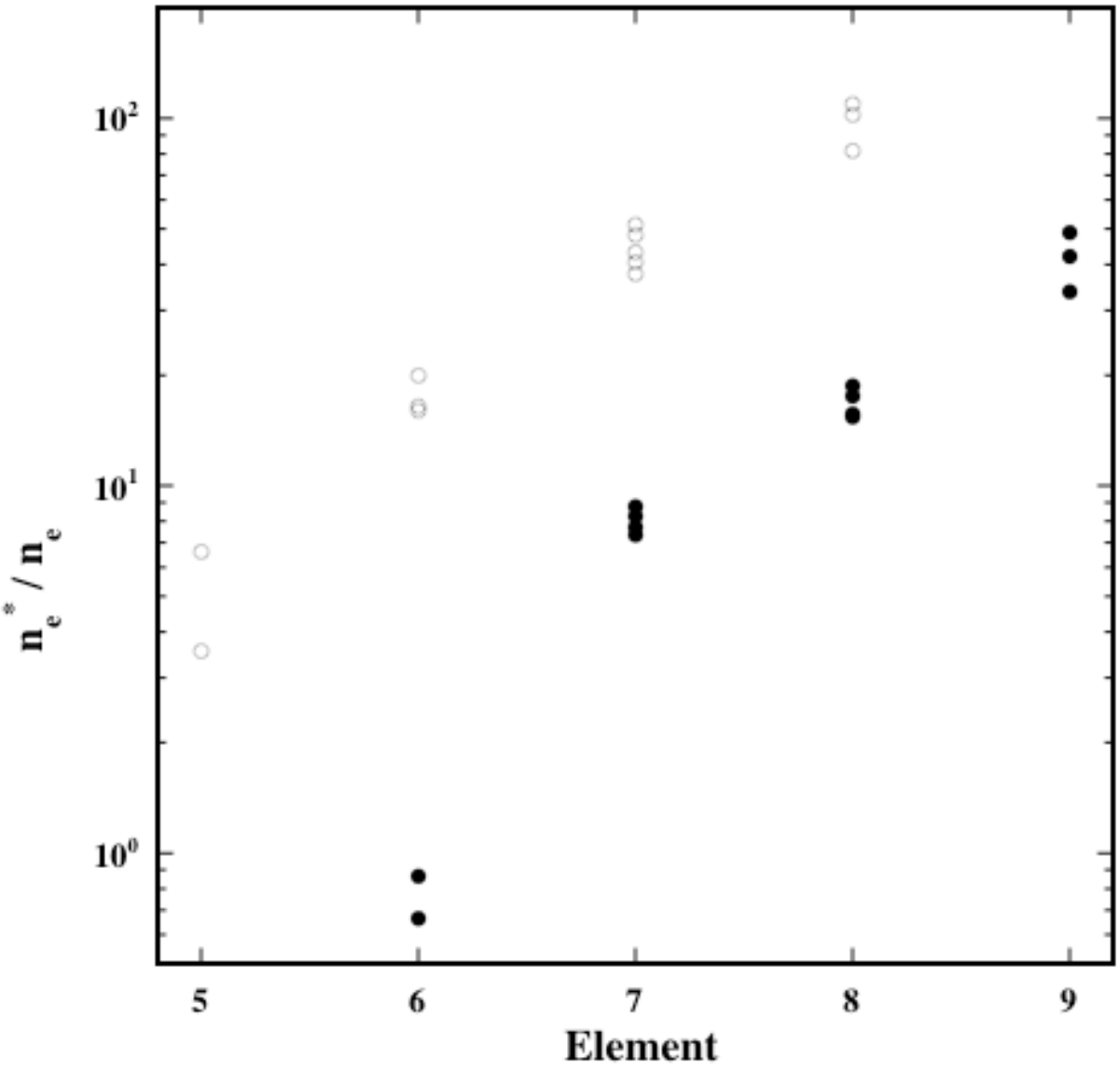
10^2
10^1
10^0
n_e^* / n_e
5
6
7
8
9
Element